

Thermal, spectroscopic and DFT studies of solid benzamide

G. L. Perpétuo², D. A. Gálico¹, R. B. Guerra¹, R. Moreira¹, G. O. Chierice², G. Bannach^{1*}

¹Faculdade de Ciências, UNESP – Universidade Estadual Paulista, Departamento de Química, CEP 17033-360, Bauru, São Paulo, Brazil

²Instituto de Química de São Carlos, Universidade de São Paulo, Av. Trabalhador são-carlense, 400 – 13560-970 São Carlos/SP, Brazil

Received 13/05/2014; accepted 29/07/2014

Available online 26/08/2014

Abstract

Thermogravimetry (TG), differential thermal analysis (DTA), differential scanning calorimetry (DSC), Fourier transform infrared spectroscopy (FTIR), and DFT theoretical calculations were used to study benzamide. The TG-DTA and DSC curves provided information concerning the melting point, evaporation and thermal stability of the compound. Using the FTIR technique it was possible to confirm the evaporation of the compound with no degradation. Density functional theory (DFT) at the 6-311⁺⁺G (3df, 3dp) level, provided information regarding the energies involved in HOMO-LUMO transitions and the chemical stability of the compound.

Keywords: Benzamide, Evaporation, FTIR

1. Introduction

Benzamide (Fig. 1) presents itself in solid form as a white powder; it also has polymorphic variations [1]. Its molecular weight is 121.14 g mol⁻¹, and its melting point is reported as 130 °C in the literature [2]. Cocrystals are multi-component solid-state assemblies of two or more compounds held together by any type or combination of intermolecular interactions [3]. Benzamide can be used for the synthesis of pharmaceutical cocrystals [4-6]. These compounds, due to their crystalline characteristics, exhibit greater stability regarding moisture and storage. Moreover, cocrystals have a lower tendency to undergo phase transformations and they are stable during the process of wet granulation, tableting, compaction, etc. [7]. These advantages can bring benefits for patients, such as a better fit during ingestion due to a better solubility of the drug, and can even decrease potential side effects [8-13].

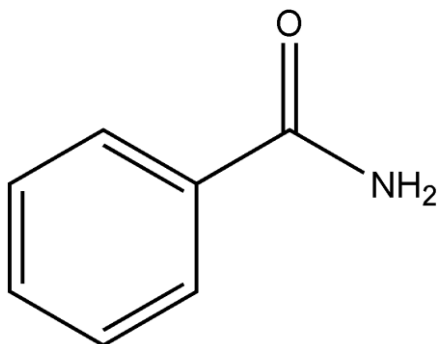


Figure 1. Structural formula of benzamide.

Using TG-DTA and DSC it is possible to monitor the effects of heat associated with specific physical or chemical samples, such as phase transitions (melting, boiling, sublimation, freezing, changes in crystal structure), or dehydration reactions, dissociation, decomposition,

oxidation-reduction, leading to heat variations [14] and also provide important information about reactions in solid [15] and kinetic reactions [16]. However, in some cases, additional investigations are necessary so that these curves can be interpreted in a more correct manner.

Previous studies using DSC [5, 6, 17] reported the melting point of benzamide at a temperature between approximately 126–129 °C, and the sublimation of the compound has been mentioned in some studies [17-19]. Even though the behavior of benzamide until the melting point has been studied through DSC, other studies have focused on its behavior after this temperature, or have used other thermal and spectroscopic methods of analysis.

The joint use of the FTIR technique and theoretical calculations such as DFT, provide important information about the structure of molecules [20-22].

Thus, this study aims to elucidate the thermal behavior of benzamide through the techniques of thermal analysis (TG-DTA and DSC) and FTIR.

2. Experimental

TG-DTA curves were obtained with SDT Q600 equipment, TA Instruments, using approximately 5 mg of benzamide in an air atmosphere with a flow rate of 100 mL·min⁻¹, heating rate 10 °C·min⁻¹, and a temperature range of 25-300 °C.

The DSC curves were obtained using DSC Q10 equipment, TA Instruments. An aluminum crucible with perforated cover was used as a sample holder; an empty similar crucible was used as a reference. The heating rate was 10 °C·min⁻¹ with a sample mass of approximately 2 mg, nitrogen flow rate of 50 mL·min⁻¹ and temperature range of 40-380 °C.

* Corresponding author: Tel.: +55 (14) 3103-7820
E-mail address: gilbert@fc.unesp.br (G. Bannach)

The FTIR spectra were obtained using a Thermo Scientific Nicolet iS5, spectrometer. The spectra were obtained by the reflectance method with a scanning range between 600 cm^{-1} and 4000 cm^{-1} (resolution 4 cm^{-1}) and a crystal of germanium as support.

X-ray powder diffractogram were measured on a Siemens DMAX 2000 x-ray diffractometer using $\text{Cu K}\alpha$ radiation ($\lambda = 1.5406\text{ \AA}$) and settings of 20 kV and 2 mA. The sample was placed in a glass support and exposed to the radiation ($3^\circ \leq 2\theta \leq 50^\circ$).

2.1. Computational strategy

In this study, the quantum chemical approach used to determine the molecular structures was the Becke three-parameter hybrid theory [23] using the Lee–Yang–Parr (LYP) functional correlation [24] and the basis set used for the calculations was the 6-311++G (3df, 3dp) [25, 26]. The molecular calculations were performed using the Gaussian 09 routine [27].

The theoretical infrared spectrum was calculated using a harmonic field [28] based on the C_1 symmetry (electronic state 1A). The frequency values (not scaled), relative intensities, assignments and description of vibrational modes are presented. The geometry optimization was processed using the Bery optimization algorithm [29] and the calculations of the vibrational frequencies were also implemented in order to determine an optimized geometry, considering the minimum and saddle points. The principal active infrared fundamental modes, assignments and descriptions were made by using the Gauss View 5.0.8 graphics program [30].

3. Results and Discussion

The TG and DTA curves of benzamide are shown in Figure 2. The TG curve shows that the benzamide was stable up to approximately $100\text{ }^\circ\text{C}$, when the fusion process started, followed by evaporation. These thermal processes can be proven by the two endothermic peaks which appear in the DTA curve. The peaks at $124\text{ }^\circ\text{C}$ and $214\text{ }^\circ\text{C}$ are attributed to the melting and the evaporation of the benzamide, respectively.

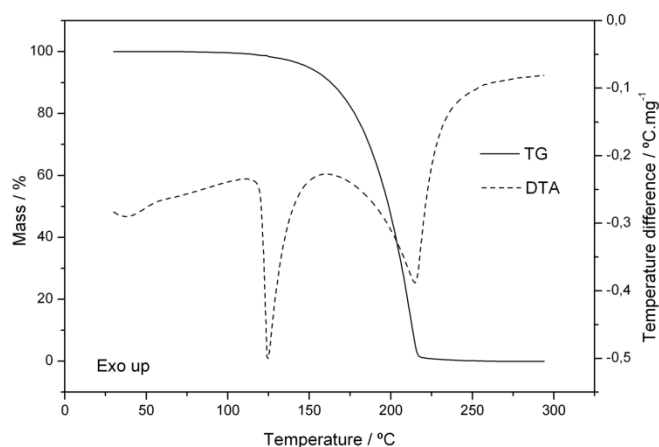


Figure 2. TG-DTA curves of benzamide.

The DSC curve (Fig. 3) shows an endothermic peak at $127\text{ }^\circ\text{C}$, which refers to the melting of the compound, with

$\Delta H = 24.31\text{ kJ.mol}^{-1}$ and 99.1% of purity, calculated according to the Van't Hoff equation. Another endothermic peak appears at $258\text{ }^\circ\text{C}$, which can be attributed to the evaporation of the compound. The peaks observed in the DSC curve are in agreement with the DTA curve. The DSC curve of Benzamide in an air atmosphere showed the same behavior of the DSC curve in a N_2 atmosphere. Thus only the DSC curve atmosphere N_2 was shown.

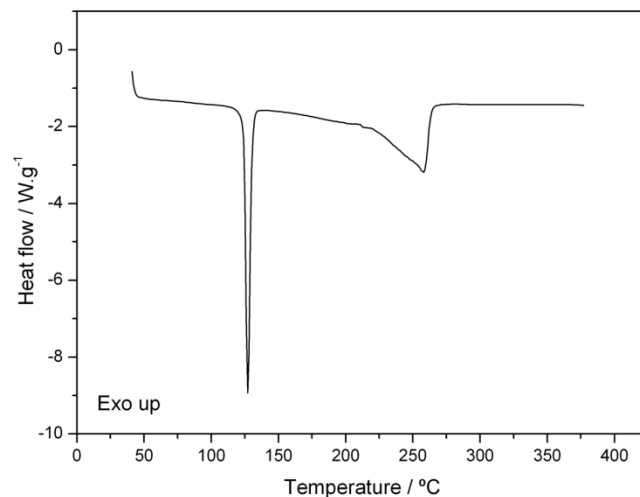


Figure 3. DSC curve of benzamide.

The TG curve suggests that the compound decomposed in a single step but the FTIR spectrum of the volatile recrystallized product (Fig. 4) confirmed that the studied compound evaporated after melting, without thermal decomposition.

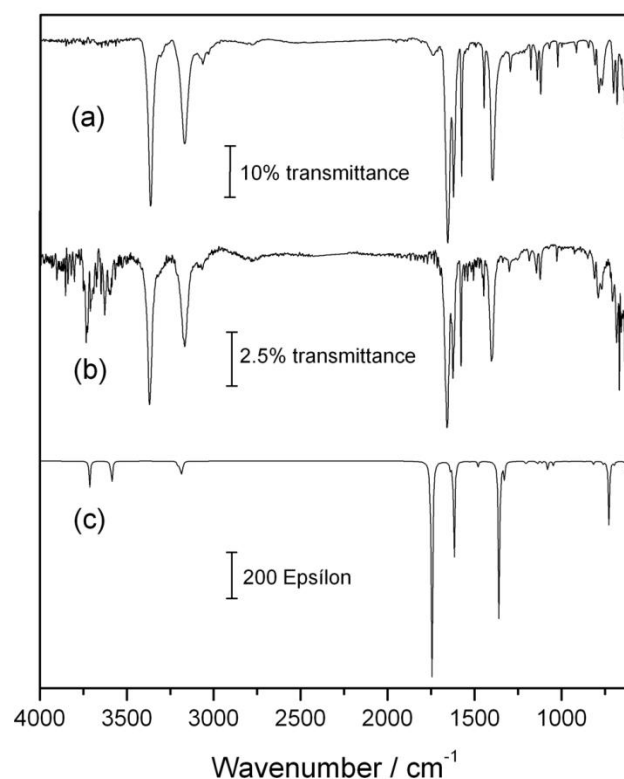


Figure 4. Comparison between (a) standard benzamide, (b) recrystallized benzamide and (c) theoretical FTIR spectra of benzamide.

The X-ray powder patterns of standard and recrystallized benzamide are shown in Fig. 5; these data suggest that a structural modification occurred after recrystallization, due to the shift or disappearance of some peaks.

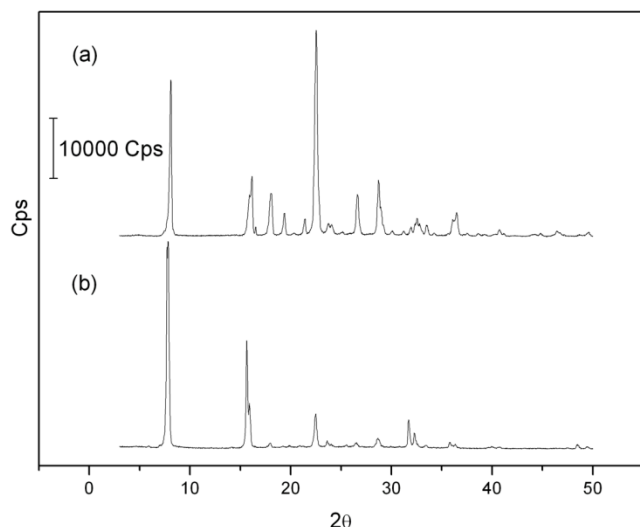


Figure 5. X-ray powder diffraction patterns of (a) standard benzamide and (b) recrystallized benzamide.

Theoretical data for the optimized benzamide structure are shown in Table 1. The theoretical infrared

spectrum helped us interpret the experimental IR spectrum and provided information about the geometric parameters of this compound. The theoretical vibrational assignments were made using Gauss View 5.0.8 [30]. In order to achieve a better agreement between the theoretical and experimental assignments, we followed a scaling factor of 0.9604 for B3LYP/6-311⁺⁺G (3df, 3dp) [31].

The infrared spectroscopic data for benzamide (theoretical and experimental) are shown in Table 2 and Fig. 4. The frontier molecular orbitals (FMOs) consist of the highest occupied molecular orbitals (HOMOs) and the lowest-lying unoccupied molecular orbitals (LUMOs); they play an important role in electric and optical properties, as well as in chemical reactions. The energy gap between the HOMOs and LUMOs characterizes the molecular chemical stability, chemical reactivity, and hardness or softness of the molecule. When a molecule has a small gap, it is more polarizable and generally has a high chemical reactivity and low kinetic stability [32, 33]. The atomic orbital compositions, the energy levels of the HOMO and LUMO orbitals, and the energy gap between the HOMO and LUMO, computed for benzamide, are shown in Fig. 6. This value of 5.611 eV (221 nm), and its assignment to a π - π^* transition between $S_0 \rightarrow S_3$, shows that it is in agreement with the experimental value and also the discussion related in the literature [34, 35].

Table 1 Theoretical data for the optimized structure of benzamide optimized using DFT/B3LYP method.

Atom #	Atom	NA	NB	NC	Bond /Å	Angle /°	Dihedral /°	X /Å	Y /Å	Z /Å
1	C							1.848027	1.224328	-0.13223
2	C	1			1.389502			0.459049	1.189515	-0.14788
3	C	2	1		1.396223	120.3913		-0.21864	-0.02409	-0.01615
4	C	3	2	1	1.395328	119.1859	-0.51732	0.516142	-1.20238	0.120433
5	C	4	3	2	1.387231	120.4118	1.018397	1.90266	-1.16632	0.146437
6	C	1	2	3	1.390007	120.0209	-0.27502	2.571505	0.047365	0.020931
7	H	1	2	3	1.081545	119.8325	179.2417	2.363908	2.167918	-0.24731
8	H	2	1	6	1.081727	119.0751	-178.15	-0.08821	2.11041	-0.2982
9	H	4	3	2	1.080472	118.4208	-178.879	-0.02059	-2.13647	0.203021
10	H	5	4	3	1.081554	119.8482	179.4953	2.462961	-2.08432	0.260896
11	H	6	1	2	1.081731	120.0055	-179.841	3.652781	0.075065	0.035654
12	C	3	2	1	1.501014	123.2134	-179.493	-1.71532	-0.13634	-0.0355
13	O	12	3	2	1.217509	121.9351	158.8737	-2.2793	-1.18328	-0.29661
14	N	12	3	2	1.368535	116.4877	-20.2051	-2.41672	1.006714	0.237197
15	H	14	12	3	1.006438	116.3539	-173.726	-3.41498	0.909261	0.320222
16	H	14	12	3	1.00396	121.2809	-18.7531	-1.98498	1.784888	0.701933

Atom# + NA = Bond; Atom# + NA + NB = Angle; Atom# + NA + NB + NC = Dihedral; X, Y and Z = atomic coordinates.

Table 2 Comparison between theoretical and experimental FTIR data of benzamide.

Assignment	Theoretical	Experimental	$\Delta\nu$ (cm ⁻¹)
ν_a NH	3566	3366	200
ν_s NH	3445	3170	275
ν CH _{ring}	3068, 3060	3066, 3032	2, 28
ν C=O + δ NH ₂ + ν CC _{ring}	1676	1656	20
δ NH ₂	1553	1625	-72
ρ_r CH _{ring}	1420	1502	-82
ν CN + ρ_r CH _{ring}	1306	1399	-93
ρ_w CH _{ring} + ρ_w NH	698	770	-72

ν , stretching; δ , scissoring; ρ_w , wagging; ρ_r , rocking; subscripts *a* and *s* denotes asymmetric and symmetric respectively.

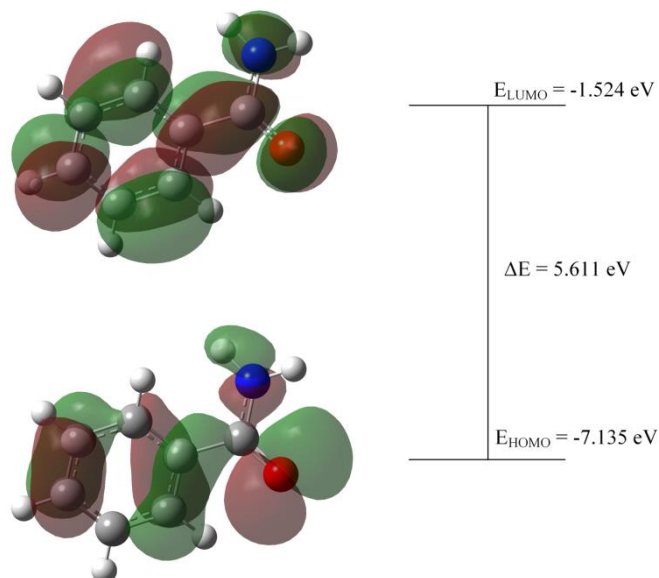


Figure 6. HOMO and LUMO molecular orbitals calculated for benzamide.

4. Conclusions

The TG-DTA curves supplied information on the thermal stability and thermal behavior of benzamide in air atmosphere. These data show that benzamide evaporates after melting, without decomposition, as confirmed by the FTIR spectra of the volatile recrystallized product. The DSC curves allowed us to determine the melting point of benzamide as well as the fusion enthalpy. The theoretical calculations helped us propose a structural model for benzamide and were important for the interpretation of the FTIR results. The energies of the HOMO and LUMO orbitals were obtained through theoretical calculations and are in agreement with the experimental values found in the literature.

Acknowledgements

The authors would like to thank the FAPESP (Proc. 2012/21450-1) and CNPq foundations (Brazil) for their financial support and Prof. Dr. Éder Tadeu Gomes Cavaleiro for allowing the use of the TG-DTA and DSC equipment. This research was supported by resources supplied by the Center for Scientific Computing (NCC/GridUNESP) of the São Paulo State University (UNESP).

References

- [1] David WIF, Shankland K, Pulham CR, Blagden N, Davey RJ, Song M. Polymorphism in Benzamide. *Angew. Chem. Int.* 2005;44(43):7032-7035. [\[Google Scholar\]](#) [\[Available from\]](#) [\[CrossRef\]](#)
- [2] The MERCK INDEX: an encyclopedia of chemicals, drugs, and biological. 13^{ed} Nova Jersey: Whitehouse Station. 2001, pp. 147. [\[Google Scholar\]](#) [\[Available from\]](#)
- [3] Bhogala BR, Nangia A. Ternary and quaternary co-crystals of 1,3-*cis*, 5-*cis*-cyclohexanetricarboxylic acid and 4,4'-bipyridines. *New J. Chem.* 2008;32(5):800-807. [\[Google Scholar\]](#) [\[Available from\]](#) [\[CrossRef\]](#)
- [4] Seaton CC, Parkin A. Making benzamide cocrystals with benzoic acids: The influence of chemical structure. *Cryst. Growth. Des.* 2011;11(5):1502-1511. [\[Google Scholar\]](#) [\[Available from\]](#) [\[CrossRef\]](#)
- [5] Elbagerma MA, Edwards HGM, Munshi T, Scowen IJ. Identification of a new co-crystal of salicylic acid and benzamide of pharmaceutical relevance. *Anal. Bioanal. Chem.* 2010;397(1):137-146. [\[Google Scholar\]](#) [\[Available from\]](#) [\[PubMed\]](#) [\[CrossRef\]](#)
- [6] Brittain HG. Vibrational spectroscopic studies of cocrystals and salts. 1. The benzamide-benzoic acid system. *Cryst. Growth. Des.* 2009;9(5):2492-2499. [\[Google Scholar\]](#) [\[Available from\]](#) [\[CrossRef\]](#)
- [7] Babu NJ, Nangia A. Solubility advantage of amorphous drug and pharmaceutical cocrystals. *Cryst. Growth. Des.* 2011;11(7):2662-2679. [\[Google Scholar\]](#) [\[Available from\]](#) [\[CrossRef\]](#)
- [8] Jung MS, Kim JS, Kim MS, Alhalaweh A, Cho W, Hwang SJ, et al. Bioavailability of indomethacin-saccharin cocrystals. *J. Pharm. Pharmacol.* 2010;62(11):1560-1568. [\[Google Scholar\]](#) [\[Available from\]](#) [\[PubMed\]](#) [\[CrossRef\]](#)
- [9] Shiraki K, Takata N, Takano R, Hayashi Y, Terada K. Dissolution improvement and the mechanism of the improvement from cocrystallization of poorly water-soluble compounds. *Pharm. Res.* 2008;25(11):2581-2592. [\[Google Scholar\]](#) [\[Available from\]](#) [\[PubMed\]](#) [\[CrossRef\]](#)
- [10] Yadav AV, Shete AS, Dabke AP, Kulkarni PV, Sakhare SS. Co-crystals: a novel approach to modify physicochemical properties of active pharmaceutical ingredients. *Indian J. Pharm. Sci.* 2009;71(4):359-370. [\[Google Scholar\]](#) [\[Available from\]](#) [\[PubMed\]](#) [\[CrossRef\]](#)
- [11] Good DJ, Hornedo NR. Solubility advantage of pharmaceutical cocrystals. *Growth. Des.* 2009;9(5):2252-2264. [\[Google Scholar\]](#) [\[Available from\]](#) [\[CrossRef\]](#)
- [12] Chieng N, Aaltonen J, Saville D, Rades T. Physical characterization and stability of amorphous indomethacin and ranitidine hydrochloride binary systems prepared by mechanical activation. *Eur. J. Pharm. Biopharm.* 2009;71(1):47-54. [\[Google Scholar\]](#) [\[Available from\]](#) [\[PubMed\]](#) [\[CrossRef\]](#)

- [13] Almarsson Ö, Zaworotko MJ. Crystal engineering of the composition of pharmaceutical phases. Do pharmaceutical co-crystals represent a new path to improved medicines. *Chem. Commun.* 2004;7(17):1889-1896. [[Google Scholar](#)] [[Available from](#)] [[PubMed](#)] [[CrossRef](#)]
- [14] Galwey AK, Craig DQM. Thermogravimetric analysis: Basic principles. In: Craig DQM, Reading M, editors. *Thermal analysis of pharmaceuticals*. New York: CRC; 2007. [[Google Scholar](#)]
- [15] Gálico DA, Holanda BB, Perpétuo GL, Schnitzler E, Treu-Filho O, Bannach G. Thermal and spectroscopic studies on solid Ketoprofen of lighter trivalent lanthanides. *J. Therm. Anal. Calorim.* 2012;108(1):371-9. [[Google Scholar](#)] [[Available from](#)] [[CrossRef](#)]
- [16] Tița B, Marian E, Fuliș A, Jurca T, Tița D. Thermal stability of piroxicam. Part 2. Kinetic study of the active substance under isothermal conditions. *J. Therm. Anal. Calorim.* 2013;112(1):367-74. [[Google Scholar](#)] [[Available from](#)] [[CrossRef](#)]
- [17] Butterhof C, Martin T, Ectors P, Zahn D, Niemietz P, Senker J, et al. Thermoanalytical evidence of metastable molecular defects in form I of benzamide. *Cryst. Growth. Des.* 2012;12(11):5365-5372. [[Google Scholar](#)] [[Available from](#)] [[CrossRef](#)]
- [18] Almeida ARRP, Monte MJS. Thermodynamic study of benzamide, N-methylbenzamide, and N,N-dimethylbenzamide: Vapor pressures, phase diagrams, and hydrogen bond enthalpy. *J. Chem. Eng. Data.* 2010;55(9):3507-3512. [[Google Scholar](#)] [[Available from](#)] [[CrossRef](#)]
- [19] Gutterman A, Rath N, Chickos J. Validation of the vaporization enthalpies of some simple aliphatic amides and their use in the evaluation of the vaporization enthalpy of valpromide and valnoctamide. *J. Chem. Eng. Data.* 2013;58(3):749-757. [[Google Scholar](#)] [[Available from](#)] [[CrossRef](#)]
- [20] Gálico DA, Perpétuo GL, Castro RAE, Treu-Filho O, Legendre AO, Galhiane MS, et al. Thermoanalytical study of nimesulide and their recrystallization products obtained from solutions of several alcohols. *J. Therm. Anal. Calorim.* 2014;115(3):2385-90. [[Google Scholar](#)] [[Available from](#)] [[CrossRef](#)]
- [21] Bannach G, Arcaro R, Ferroni DC, Siqueira AB, Treu-Filho O, Ionashiro M, et al. Thermoanalytical study of some anti-inflammatory analgesic agents. *J. Therm. Anal. Calorim.* 2010;102(1):163-70. [[Google Scholar](#)] [[Available from](#)] [[CrossRef](#)]
- [22] Perpétuo GL, Gálico DA, Fugita RA, Castro RAE, Eusébio MES, Treu-Filho O, et al. Thermal behavior of some antihistamines. *J. Therm. Anal. Calorim.* 2013;111(3):2019-28. [[Google Scholar](#)] [[Available from](#)] [[CrossRef](#)]
- [23] Becke AD. Density-functional thermochemistry. III. The role of exact exchange. *J. Chem. Phys.* 1993;98(7):5648-5652. [[Google Scholar](#)] [[Available from](#)] [[CrossRef](#)]
- [24] Lee C, Yang W, Parr RG. Development of the colle-salvetti correlation-energy formula into a functional of the electron density. *Phys Rev B* 1988;37(2):785-789. [[Google Scholar](#)] [[Available from](#)] [[CrossRef](#)]
- [25] McLean AD, Chandler GS. Contracted Gaussian-basis sets for molecular calculations. 1. 2nd row atoms, Z=11-18. *J. Chem. Phys.* 1980;72(10):5639-5648. [[Google Scholar](#)] [[Available from](#)] [[CrossRef](#)]
- [26] Raghavachari K, Binkley JS, Seeger R, Pople JA. Self-Consistent Molecular Orbital Methods. XX. Basis set for correlated wave-functions. *J. Chem. Phys.* 1980;72(1):650-654. [[Google Scholar](#)] [[Available from](#)] [[CrossRef](#)]
- [27] Gaussian 09, Revision **D.01**, Frisch MJ; Trucks GW; Schlegel HB; Scuseria GE; Robb MA; Cheeseman JR; Scalmani G; Barone V; Mennucci B; Petersson GA; Nakatsuji H; Caricato M; Li X; Hratchian HP; Izmaylov AF; Bloino J; Zheng G; Sonnenberg JL; Hada M; Ehara M; Toyota K; Fukuda R; Hasegawa J; Ishida M; Nakajima T; Honda Y; Kitao O; Nakai H; Vreven T; Montgomery JA Jr; Peralta JE; Ogliaro F; Bearpark M; Heyd JJ; Brothers E; Kudin KN; Staroverov VN; Kobayashi R; Normand J; Raghavachari K; Rendell A; Burant JC; Iyengar SS; Tomasi J; Cossi M; Rega N; Millam MJ; Klene M; Knox JE; Cross JB; Bakken V; Adamo C; Jaramillo J; Gomperts R; Stratmann RE; Yazyev O; Austin AJ; Cammi R; Pomelli C; Ochterski JW; Martin RL; Morokuma K; Zakrzewski VG; Voth GA; Salvador P; Dannenberg JJ; Dapprich S; Daniels AD; Farkas Ö; Foresman JB; Ortiz JV; Cioslowski J; Fox DJ. *Gaussian, Inc., Wallingford CT, 2009.* [[Google Scholar](#)] [[Available from](#)]
- [28] Goodson DZ, Sarpal SK, Bopp P, Wolfsberg M. Influence on isotope effect calculations of the method of obtaining force constants from vibrational data. *J. Phys. Chem.* 1982;86(5):659-663. [[Google Scholar](#)] [[Available from](#)] [[CrossRef](#)]
- [29] Schelegel HB. In: Bertran J, editor. *New theoretical concepts for understanding organic reactions*. The Netherlands: Academic; 1989. [[Google Scholar](#)] [[Available from](#)] [[CrossRef](#)]

- [30] GaussView, Version 5.0.8, Dennington R, Keith T, Millam J. Semichem Inc., Shawnee Mission KS; 2000-2008. [\[Google Scholar\]](#) [\[Available from\]](#)
- [31] Anderson MP, Uvdal P. New scale factors for harmonic vibrational frequencies using the B3LYP density functional method with the triple- ζ basis set 6-311+G(d,p). *J. Phys. Chem. A* 2005;109(12):2937-2941. [\[Google Scholar\]](#) [\[Available from\]](#) [\[CrossRef\]](#)
- [32] Fleming I. Frontier orbitals and organic chemical reactions. New York: John Wiley and Sons; 1976. [\[Google Scholar\]](#)
- [33] Mariappan G, Sundaraganesan N, Manoharan S. The spectroscopic properties of anticancer drug apigenin investigated by using DFT calculations, FT-IR, FT-Raman and NMR analysis. *Spectrochim. Acta. A: Mol. Bio. Spectr.* 2012;95:86-99. [\[Google Scholar\]](#) [\[Available from\]](#) [\[PubMed\]](#) [\[CrossRef\]](#)
- [34] Liler M. Spectrophotometric confirmation of the tautomerism of bide cations in concentrated sulphuric acid. *JCS Chem. Comm.* 1972;9:527-528. [\[Google Scholar\]](#) [\[Available from\]](#) [\[CrossRef\]](#)
- [35] Artyukhov VY, Morev AV. Quantum-chemical investigation of spectral-luminescent and physical-chemical properties of benzamides. *Russ. Phys. J.* 2003;46(5):488-492. [\[Google Scholar\]](#) [\[Available from\]](#) [\[CrossRef\]](#)